BioResearch Open Access
Volume 3, Number 6, December 2014

DOI: 10.1089/biores.2014.0050

In Vivo Ectopic Bone Formation by Devitalized Mineralized Stem Cell Carriers Produced Under Mineralizing Culture Condition

Yoke Chin Chai,[1–3] Liesbet Geris,[3,4] Johanna Bolander,[1,3] Grzegorz Pyka,[3,5] Simon Van Bael,[3,6] Frank P. Luyten,[1,3,*] and Jan Schrooten[3,5,*]

Abstract

Functionalization of tissue engineering scaffolds with *in vitro*–generated bone-like extracellular matrix (ECM) represents an effective biomimetic approach to promote osteogenic differentiation of stem cells *in vitro*. However, the bone-forming capacity of these constructs (seeded with or without cells) is so far not apparent. In this study, we aimed at developing a mineralizing culture condition to biofunctionalize three-dimensional (3D) porous scaffolds with highly mineralized ECM in order to produce devitalized, osteoinductive mineralized carriers for human periosteal-derived progenitors (hPDCs). For this, three medium formulations [i.e., growth medium only (BM1), with ascorbic acid (BM2), and with ascorbic acid and dexamethasone (BM3)] supplemented with calcium (Ca^{2+}) and phosphate (PO_4^{3-}) ions simultaneously as mineralizing source were investigated. The results showed that, besides the significant impacts on enhancing cell proliferation (the highest in BM3 condition), the formulated mineralizing media differentially regulated the osteochondro-related gene markers in a medium-dependent manner (e.g., significant upregulation of *BMP2*, bone sialoprotein, osteocalcin, and *Wnt5a* in BM2 condition). This has resulted in distinguished cell populations that were identifiable by specific gene signatures as demonstrated by the principle component analysis. Through devitalization, mineralized carriers with apatite crystal structures unique to each medium condition (by X-ray diffraction and SEM analysis) were obtained. Quantitatively, BM3 condition produced carriers with the highest mineral and collagen contents as well as human-specific VEGF proteins, followed by BM2 and BM1 conditions. Encouragingly, all mineralized carriers (after reseeded with hPDCs) induced bone formation after 8 weeks of subcutaneous implantation in nude mice models, with BM2-carriers inducing the highest bone volume, and the lowest in the BM3 condition (as quantitated by nano-computed tomography [nano-CT]). Histological analysis revealed different bone formation patterns, either bone ossicles containing bone marrow surrounding the scaffold struts (in BM2) or bone apposition directly on the struts' surface (in BM1 and BM3). In conclusion, we have presented experimental data on the feasibility to produce devitalized osteoinductive mineralized carriers by functionalizing 3D porous scaffolds with an *in vitro* cell-made mineralized matrix under the mineralizing culture conditions.

Key words: biomineralization; bone regeneration; devitalization; mineralized extracellular matrix; osteoinductive carriers

Introduction

A SUCCESSFUL REPAIR OF DEFECTED tissue/organ via tissue engineering approach requires the engineering of constructs with a high degree of biomimetic modalities that recapitulate the native tissue developmental process in an *in vivo* recognizable and bioinstructive manner.[1,2] These requirements represent a unique scientific art to ''decorate'' synthetic constructs *in vitro* with crucial biological entities that could timely promote construct viability, direct tissues

[1]Tissue Engineering Laboratory, Skeletal Biology and Engineering Research Center, KU Leuven, Leuven, Belgium.
[2]Department of Biomedical Engineering, Faculty of Engineering, University of Malaya, Kuala Lumpur, Malaysia.
[3]Prometheus, Division of Skeletal Tissue Engineering, KU Leuven, Leuven, Belgium.
[4]Biomechanics Research Unit, University of Liege, Liege, Belgium.
[5]Department of Materials Engineering, and [6]Division of Production Engineering, Machine Design and Automation, Department of Mechanical Engineering, KU Leuven, Heverlee, Belgium.
*Shared senior authorship: Jan Schrooten and Frank P. Luyten.

growth, and subsequently integrate and function within the host system. However, development of such ''intelligent'' construct is both scientifically and technologically challenging[3] due to the high complexity of a biological system, and hence hinders the identification of key biological elements and their sequential events that are to be engineered.[4]

Recently, whole organ-derived decellularized extracellular matrix (ECM) has been explored as a native building block to facilitate tissue/organ regeneration by combining it with stem cells.[5] It is hypothesized that the native ECM provides a natural biological framework containing the necessary bioactive motifs and microenvironment niche that favor tissue growth.[6] Indeed, this approach has shown reactivation of specific organ functionalities, such as the *in vitro* ''beating'' of a heart after repopulating a decellularized heart with predifferentiated contractile cells.[7] Nevertheless, this approach is not novel in the field of skeletal repair, where demineralized bone matrix (DBM) has a long clinical track record as bone filler[8,9] and has also been widely investigated as a tissue engineering carrier for bone defect repair.[10–12] Unfortunately, the use of DBM (either xeno- or allogeneic) has several drawbacks.[8] To overcome these, scientists have resorted to use *in vitro* cell culture–derived mineralized ECM as possible alternative osteoinductive motif to functionalize three-dimensional (3D) porous scaffolds.[13] In fact, enhanced osteogenic differentiation *in vitro* has been reported[14,15]; however, the bone-forming capacity is so far not apparent.[16,17]

It is known that bone matrix consists of mineralized collagen fibers embedded with essential growth factors and trace elements. This matrix is produced by osteoblastic cells through specific physiological events,[18,19] giving rise to a unique biological architecture and mineralization hierarchy[20,21] that governs its functionality and osteoinductivity.[22] Introducing all these biomimetic features in a controlled way through synthetic processing routes (such as biomimetic deposition in simulated body fluid,[23,24] electrolytic deposition,[25,26] plasma spraying,[27,28] and sol-gel[29,30] techniques) remains challenging, mainly due to the lack of in-depth knowledge on the biological events and the limitations of existing technological tools.[31–33] Recently, we have reported the feasibility to use either Ca^{2+} or PO_4^{3-} supplementation to produce living 3D osteogenic hybrids *in vitro*.[34] However, simultaneous use of Ca^{2+} and PO_4^{3-} as mineralizing sources to functionalize a bio-inert scaffold with highly mineralized ECM in order to produce devitalized osteoinductive stem cells carriers has not been explored. Therefore, in this study we aimed at developing a so-called biomineralization medium (BM) to promote *in vitro* cell proliferation, osteogenic differentiation, and high bone-like ECM deposition on 3D porous scaffolds. We anticipate that this approach may facilitate the production of robust biomimetic mineralized carriers enriched with natural cell adhesion peptides and osteoinductive motifs that are minimally required to effectively emulate bone-specific cell–ECM interactions, eventually leading to osteogenesis preceded by matrix remodeling.

To test this hypothesis, simultaneous Ca^{2+} and PO_4^{3-} supplementation in three medium formulations [i.e., in growth medium (BM1), growth medium plus ascorbic acid (BM2), and growth medium plus ascorbic acid plus dexamethasone (BM3); Table 1] were investigated using human periosteal-derived progenitors (hPDCs) seeded on 3D open porous, bio-inert Ti6Al4V (Ti)-scaffolds produced by additive manufacturing. This includes 3D hPDC proliferation and osteochondro-related gene marker expression. After devitalization, the microscopic mineral morphology, composition, and the presence of growth factors in the matrix extracts were assessed. The ectopic bone-forming capacity was evaluated by subcutaneous implantation of hPDC-reseeded mineralized carriers in nude mice for 8 weeks followed by nano-CT quantification and histological analysis.

Table 1. Composition of the Investigated Biomineralization Media as Compared to the Control Medium (GM′ or OM^-) Without Ca^{2+} and PO_4^{3-} Supplementation

Treatment	*Growth medium*	*Ascorbic acid (50 μg/ml)*	*Dexamethasone (100 nM)*	*6 mM Ca^{2+} + 4 mM PO_4^{3-}*
GM′	+	+	−	−
OM^-	+	+	+	−
BM1	+	−	−	+
BM2	+	+	−	+
BM3	+	+	+	+

''+'' and ''−'' indicate the presence and absence of the respective chemical compounds.

BM, biomineralization media; GM, growth medium.

Materials and Methods

Materials

Calcium chloride ($CaCl_2 \cdot 6H_2O$; Applichem), sodium dihydrogen phosphate dihydrate ($NaH_2PO_4 \cdot 2H_2O$; Merck), di-sodium hydrogen phosphate dehydrate ($Na_2HPO_4 \cdot 2H_2O$; Merck), dexamethasone (Sigma-Aldrich), and L-ascorbic acid 2-phosphate sesquimagnesium hydrate (Sigma-Aldrich) were purchased from the manufacturers. Center hollow (diameter 2 mm), diamond unit cell, 3D open porous Ti6Al4V (Ti)-scaffolds (diameter 6 mm × height 3 mm; pore size 1000 μm; porosity 93%) were designed using Magics software (Materialise N.V.) and produced by selective laser melting.[35] The scaffolds were then cleaned with acetone, 96% ethanol, and demineralized water (each for 15 min) using ultrasonic bath, followed by oxidation in 5 M NaOH at 60°C for 24 h and finally rinsed thoroughly with demineralized water before sterilized by autoclaving. Prior to cell seeding, the sterilized scaffolds were prewetted with culture medium containing 10% fetal bovine serum (FBS) for 2 h, and dried overnight in laminar flow under sterile condition. Using computed tomography and image analysis techniques, the sterilized scaffolds were reported to have an average pore size of around 822 μm and an average porosity of 81%.[34]

In vitro *seeding and growth of hPDCs cultured on Ti-scaffolds in various BM*

Periosteal biopsies were harvested from the proximal tibia of adolescent and adult patients during total knee replacement surgery or distraction osteogenesis with patient informed consent and approval by the ethics committee for Human Medical Research of the University of Leuven. Briefly, after overnight digestion of the biopsies in culture medium containing 0.2% type

IV collagenase (Invitrogen) at 37°C, hPDCs were collected by centrifugation and subsequently expanded in growth medium (DMEM + 10% FBS + 1% antibiotics/antimycotics + 1% sodium pyruvate) using T-175 cm^2 flasks. From passage 3 onward, the expanded cells were pooled together and stored in liquid nitrogen. This cell type was reported by our research group to have fibroblastic characteristic and possesses multipotent differentiation capacity of the mesenchymal stem cell (MSC).[36]

For all assays in this study, hPDC pooled cells at early passage 4 (known to have higher homogeneity of MSC phenotype and retains bone-forming capacity) were thawed from liquid nitrogen and expanded in growth medium using T-175 cm^2 flask. Upon confluence, the cells were harvested and drop-seeded onto each scaffold (200,000 cells per scaffold), and incubated for 1 h to allow cell attachment before transferred to a rotator for overnight incubation in a cell culture incubator. This cell seeding number was optimized in-house to allow for the observation of cell proliferation and ECM deposition on these particular scaffolds within the stipulated culture time under the influence of the different medium used. Then, the samples were transferred to 12-well suspension plate and cultured dynamically using a 3D rotator (30 rpm, Grant-Bio, UK). Calcium (Ca^{2+}) and phosphate (PO_4^{3-}) solutions (600 and 400 mM, respectively) were prepared as described previously[37] and diluted 100 times in the three medium formulations with the nomenclatures shown in Table 1. Cell proliferation in each medium was assessed over 21 days of culture period by measuring the metabolic activity using AlamarBlue (10% in growth medium, Invitrogen) ($n = 3$), and DNA content using Quant-iT PicoGreen dsDNA assay (Invitrogen) ($n = 3$). Cell viability of hPDCs after 21 days of cultured under different biomineralization media was qualitatively assessed using the LIVE-DEAD viability assay kit (Life Technologies). Non-ion-supplemented growth medium containing 50 μg/ml ascorbic acid (GM′), or growth medium containing 50 μg/ml ascorbic acid and 100 nM dexamethasone (OM^-) were used for comparison purposes.

Gene expression analysis of hPDCs 3D cultures by quantitative real-time polymerase chain reaction

The expression of osteochondro-related gene markers by hPDCs after cultured in various BM for 21 days was assessed by quantitative real-time polymerase chain reaction (qRT-PCR; $n = 3$). Briefly, cells were harvested in RLT buffer and the total RNA of each sample was extracted using the RNeasy mini kit (Qiagen) as per manufacturer's instructions. The amount of extracted RNA was measured using NanoDrop (Thermo Scientific) and 500 ng of total RNA from each sample was converted to cDNA using RevertAid First Strand cDNA Synthesis kit (Thermo Scientific). qRT-PCR was cycled in a sequence detector (Rotor-Gene 6000; Corbett Life Science) using SYBR Green primers as shown in Table 2. Each sample was assessed in duplicate and compared with the housekeeping gene β-actin expression (F5′-CCCAGATCATGTTTGAGA CCT-3′; R5′-CCTCGTAGATGGGCACAGT-3′). Relative differences in expression were calculated using the $2^{-\Delta CT}$ method, and statistical significance was calculated by comparing to the $2^{-\Delta CT}$ of control medium (i.e., GM′). In order to obtain more comprehensive statistical information on the effects of BM treatments on gene expression, principle component analysis (PCA) was performed by loading the obtained gene expression data to the JMP analytical software (SAS Institute Inc.). Then, a scatterplot was produced to visualize the specific gene signatures that represent the induced cell populations after the treatments.

Production of mineralized carriers by devitalization and the mineralized ECM composition analysis

After 21 days of culture in various BM, the samples were rinsed twice with phosphate buffered saline (Bio-Whittaker) and stored at −80°C in demineralized water under sterile condition. To obtain devitalized mineralized carriers, the samples were thawed from −80°C to 37°C and then subjected to three cycles of freeze–thaw between liquid nitrogen and 37°C water bath (10 min each), followed by air-drying overnight under sterile condition. Then, the devitalized mineralized carriers were stored at −20°C under sterile condition till further analysis. The mineral phase, chemical composition, and microscopic morphology were characterized by X-ray diffraction (XRD) analysis (Seifert XRD 3003 TT; using a Cu K source in the 20–50° 2θ range; step size = 0.02°; slit size = 0.5 mm) and scanning electron microscopy coupled with energy dispersive X-ray analysis (SEM-EDAX, XL30 FEG system; Philips) at 10 kV, respectively. The amount of collagen and mineral contents deposited on Ti-scaffolds

Table 2. Primer Sequences Used for Gene Expression Analysis by Quantitative Real-Time Polymerase Chain Reaction

Gene	*Forward sequence*	*Reverse sequence*
Runx2	5′-CGCATTCCTCATCCCAGTAT-3′	5′-GCCTGGGGTCTGTAATCTGA-3′
Osx	5′-AGTGACCTTTCAGCCTCCAA-3′	5′-GGGAAAAGGGAGGGTAATCA-3′
OCN	5′-GTGCAGCCTTTGTGTCCAA-3′	5′-GCTCACACACCTCCCTCCT-3′
BMP2	5′-GTACGCAGGCACTCAGGTC-3′	5′-TTTTCCCACTCGTTTCTGGT-3′
Wnt5a	5′-GCTCCGCTCGGATTCCTC-3′	5′- CCAATGGACTTCTTCATGGCG-3′
VEGF	5′-TGCAGATTATGCGGATCAAACC-3′	5′-TGCATTCACATTTGTTGTGCTGTAG-3′
BSP	5′- GCCAGAGGAAGCAATCACCA-3′	5′- TCATTGAGAAAGCACAGGCCA-3′
Col1	5′-GACGAAGACATCCCACCAAT-3′	5′-AGATCACGTCATCGCACAAC-3′
Col2	5′-GGCTTCCATTTCAGCTATGG-3′	5′-AGCTGCTTCGTCCAGATAGC-3′
ALP	5′-GGACATGCAGTACGAGCTGA-3′	5′-GTCAATTCTGCCTCCTTCCA-3′
RankL	5′-CATCCCATCTGGTTCCCATAA-3′	5′-GCCCAACCCCGATCATG-3′
OPG	5′-GGGGACCACAATGAACAACT-3′	5′-AGCTGATGAGAGGTTTCTTCG-3′

under different medium conditions was assessed quantitatively using Picro-Sirius Red (1 mg/ml Sirius Red in saturated Picric acid, $n=3$) and Alizarin Red solutions ($n=3$).[34]

Detection of secreted human-specific VEGF proteins by Western blots

Devitalized mineralized carriers were thawed to room temperature and the mineralized matrices were extracted from the Ti-scaffolds using protein extraction buffer (0.3 M PMSF and Protease Inhibition Cocktail; Sigma) under sonication on an ice bath. For each condition, extracts from three samples were pooled and the protein concentrations were determined using the Pierce BCA Protein Assay Kit (Thermo Scientific). Then, 5 μg of extracted proteins was loaded onto a NuPAGE 4–12% Bis-Tris gel (Invitrogen) and thereafter transferred to a polyvinylidene fluoride membrane. The membranes were incubated with primary antibody–goat polyclonal anti-human $VEGF_{165}$ (1:1000; R&D Systems) according to the manufacturer's instructions. HRP-conjugated secondary antibody (Jackson) was used at a dilution of 1:2000 and images were developed by an LAS3000 Imaging System (FUJI) following the application of SuperSignal West Femto reagent (Thermo Scientific). Densitometry analysis was performed using Bio-Rad Quantity One software. Monoclonal antibody glyceraldehyde-3-phosphate dehydrogenase (GAPDH) (1:1000; Abcam) was used to assess equal loading of proteins and to quantify relative intensity of protein bands.

In vivo *ectopic implantation of hPDC-reseeded mineralized carriers*

The bone-forming capacity of the mineralized carriers produced under each culture conditions was evaluated by implantation of hPDC-reseeded mineralized carriers in NMRI-nu mice (female, 8 weeks) (three implants per mouse). Briefly, 35 μl of cell suspension containing 2 million hPDCs at passage 4 (being the minimal cell number bench mark used within our research group that is calculated based on the corresponding scaffold volume to ensure bone formation *in vivo*) was drop-seeded onto each carrier and incubated for 1 h to allow cell attachment. Then, an additional 1 ml of growth medium was added and the samples were incubated overnight on a rotator at 30 rpm before implantation in subcutaneous pockets of the mice. The implantation procedures were approved by the local ethics committee for animal research (KU Leuven) and adhered to the regulations of animal housing according to the guidelines of the KU Leuven Animalium.

Characterization of ectopic bone formation by nanofocus X-ray computed tomography and histological analysis

After 8 weeks of implantation, the samples were retrieved and fixed in 4% paraformaldehyde solution for 2 h and stored in phosphate buffered saline prior to nanofocus X-ray computed tomography (nano-CT) analysis using Phoenix Nanotom S system (GE Measurement and Control Solutions). The explants were scanned at an isotropic voxel size $(3.125\,\mu m)^3$ using a tungsten target with the following parameters: voltage = 90 kV, current = 170 μA, filter = 1 mm aluminum and 0.3 mm copper, exposure time = 500 ms, frame averaging = 1, scanning time per sample = 20 min. Image reconstruction was performed and analyzed using CTAn software (Skyscan NV), by applying an in-house algorithm involving multilevel thresholding, despeckling, and morphological operation with dilation of scaffold volume in order to eliminate the partial volume effect of the metallic materials and to segment out the bone area for quantification of bone volume. Then, the quantified bone volumes were subtracted with the background values quantified for the controls (explants of nonmineralized carriers obtained from GM′ culture condition). For histological analysis, the explants were embedded in poly-methyl methacrylate resin, sectioned using a diamond saw (Leica), and ground to approximately 70-μm-thick tissue sections. Stevenel's Blue & Van Gieson's picrofuchsin staining was used to stain the bone and soft tissue structures.

Statistical analysis

All experiments were carried out in triplicate to assess statistical significance, and the data are depicted as mean ± standard deviation (SD). Unpaired Student *t*-test (two-tailed) was performed to compare means of two groups, whereas one-way analysis of variance (ANOVA) followed by *post-hoc* Tukey's honest significant difference was used to perform multiple comparisons between the means of the experimental conditions and the controls at each time point, by establishing the statistical significance at $p<0.05$. Statistical significance is represented as follows: $^{*}p<0.05$, $^{\#}p<0.01$, and $^{\S}p<0.001$.

Results

In vitro *hPDC growth on 3D porous Ti-scaffolds in the three formulated BM*

As shown in Figure 1A, simultaneous Ca^{2+} and PO_4^{3-} supplementation into growth medium (i.e., BM1) resulted in the lowest metabolic activity over the 28 days of culture. However, the metabolic activity was significantly enhanced (especially at the later time points; $p<0.05$) in the presence of ascorbic acid (i.e., BM2) as compared to the control medium (i.e., GM′). In fact, the metabolic activity in BM2 reached a level that was comparable to culture condition containing dexamethasone and ascorbic acid (i.e., OM^-) at 28 days. Encouragingly, culturing hPDCs in BM3 (supplemented with the ions, ascorbic acid, and dexamethasone) resulted in the highest metabolic activity over 28 days ($p<0.001$ for each time point, respectively, as compared to the control medium, GM′). These data were confirmed by the total DNA content measurement on samples harvested at 28 days, where BM1 resulted in a significantly lower DNA content ($p<0.01$), and BM2 and BM3 resulted in 1.5-fold ($p<0.01$) and 2.3-fold ($p<0.001$) higher DNA content than GM′, respectively (Fig. 1B). Brightfield microscopy showed complete closure of the scaffold pores by mineralized culture (*) under BM3 culture condition, and in a lesser extent for BM1 and BM2 conditions (Fig. 1C). No mineralization of cell cultures was observed in the control media (for both GM′ and OM^-). On the other hand, live–dead staining showed high cell viability in BM2 and BM3 conditions (as indicated by high green fluorescence-labeled cells), and relatively more dead cells (red fluorescence-labeled cells, ↑) were observed in BM1 condition.

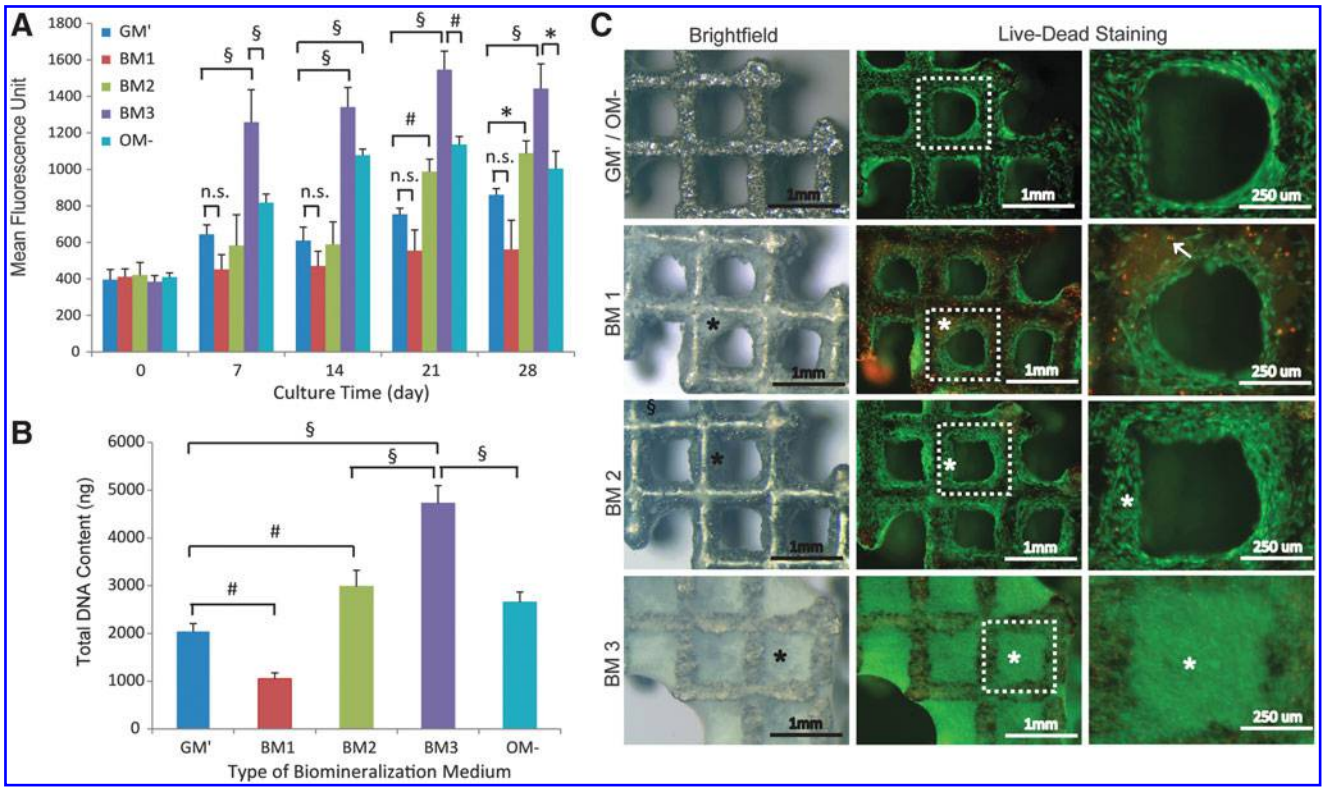

FIG. 1. *In vitro* human periosteal-derived progenitor (hPDC) growth on Ti-scaffolds in different biomineralization medium (BM). **(A, B)** The kinetics of metabolic activity over 28 days of culture and the total DNA content at 28 days, as compared to the controls (i.e., GM′ and OM^{-}). **(C)** The representative brightfield and fluorescence images showing different extent of mineralization of hPDC cultures (*) and the living (stained green) and dead cells (stained red, ↑). Mean ± SD ($n = 3$). One-way analysis of variance (ANOVA) and *post-hoc* Tukey's multiple comparison test: $^{*}p < 0.05$, $^{\#}p < 0.01$, $^{\S}p < 0.001$; n.s. = not significant.

In vitro *osteochondro-related gene markers expressions by hPDC on Ti-Scaffolds in the three formulated BM*

The effects of the formulated BM on osteogenic differentiation, bone-like matrix production, and osteoclastic recruitment activity were assessed at gene expression level by qRT-PCR after 21 days of culture, as shown in Figure 2. The results showed that simultaneous Ca^{2+} and PO_4^{3-} supplementation into the three culture media upregulated osteogenic differentiation markers, that is, osterix and *Runx2*, as compared to the control medium, that is, GM′ (Fig. 2A). Interestingly, osterix expression was most significantly upregulated ($p < 0.01$) by the ion supplementation (i.e., BM1), but was reduced in the presence of ascorbic acid (i.e., BM2) and dexamethasone (i.e., BM3). In contrast, ion supplementation along with ascorbic acid and dexamethasone (i.e., BM3) enhanced *Runx2* expression ($p < 0.01$), which was significantly higher than the BM1 condition ($p < 0.05$). Additionally, bone sialoprotein (*BSP*), an osteogenic differentiation and bone matrix marker, was highly upregulated in the BM2 condition ($p < 0.001$), but was differentially downregulated in the BM3 condition ($p < 0.05$) as compared to GM′.

Although osteocalcin (*OCN*) expression was increased in BM2, it was not significantly different from the expression in GM″, and the expression in BM1 but was significantly higher than that of BM3 ($p < 0.05$). *BMP2* expression was found to be significantly enhanced in the BM1 ($p < 0.05$) and BM2 ($p < 0.01$) conditions, but no significant difference was found between the expression in BM3 and GM′ conditions. Similarly, noncanonical Wnt ligand, that is, *Wnt5a*, was significantly enhanced in BM1 and BM2 as compared to BM3 and GM′ conditions ($p < 0.01$ for both cases). Furthermore, gene expression analysis revealed a downregulation of *Col1* and *ALP* expressions in all the three BM as compared to the control media (GM′), with no significant effect on *Col2* (Fig. 2B). Finally, culturing hPDCs in BM1 induced the highest osteoclastic recruitment activity (as indicated by the *RankL*:*OPG* ratio), followed by the BM2 condition, mainly due to a significant increase in *RankL* expression along with a significant decrease in the *OPG* expression in BM1 and BM2 as compared to GM′ condition (Fig. 2C).

PCA of the gene marker expression

Complementary, PCA showed that individual samples under the same BM culture condition could be clustered together according to their gene expression profile. Additionally, each culture condition resulted in genetically distinguishable cell populations (as indicated by the distances between the cell populations on the PCA plot [Fig. 3A]) with highly upregulated specific gene signatures (Fig. 3B). Specifically, BM1 treatment induced a cell population that had a high *RankL*:*OPG* ratio and

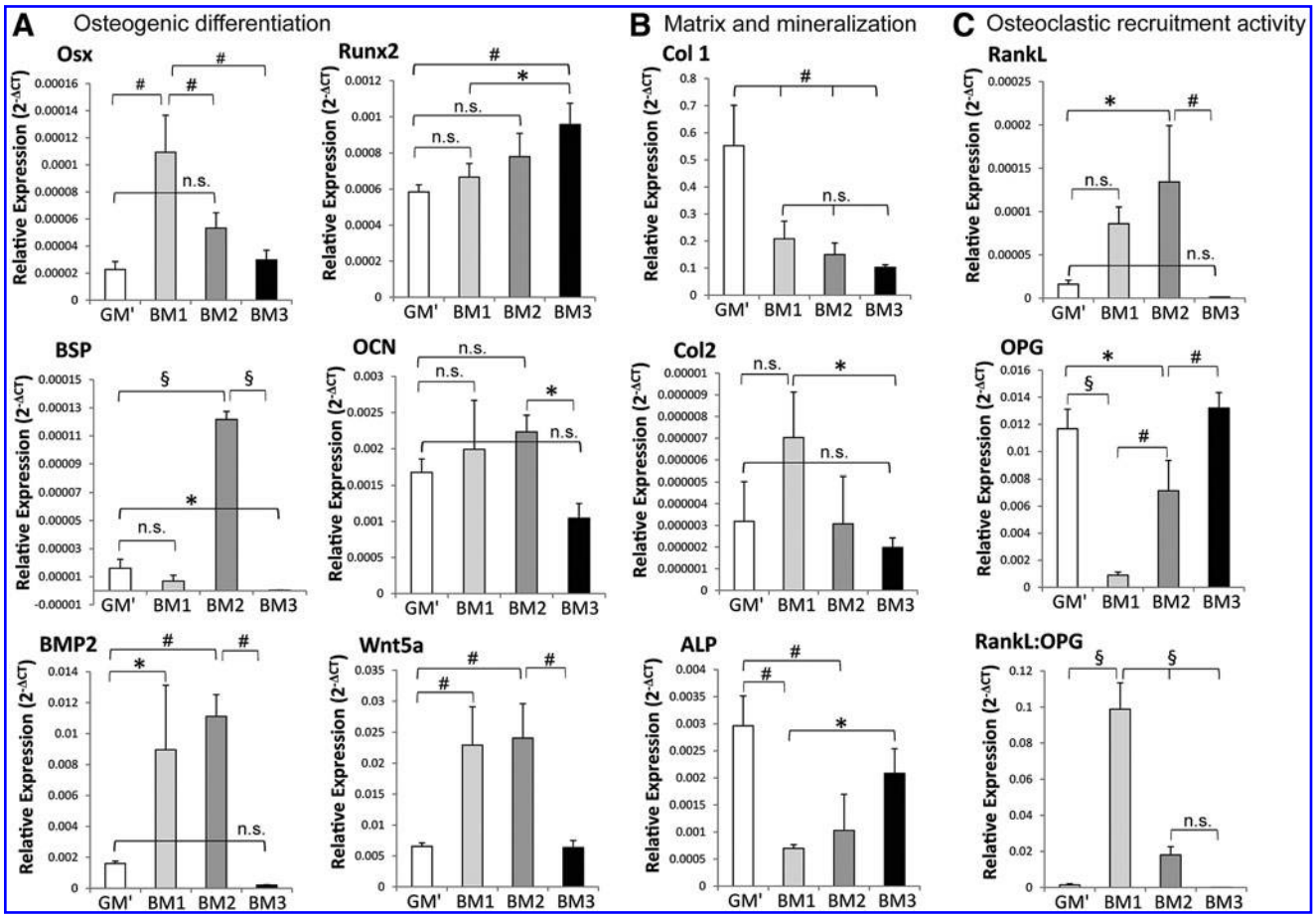

FIG. 2. *In vitro* osteogenic-related markers' expression of hPDCs on Ti-scaffolds after cultured in various BM conditions for 21 days. **(A)** Osteogenic differentiation markers: osterix (*Osx*), Runt-related transcription factor-2 (*Runx2*), bone sialoprotein (*BSP*), osteocalcin (*OCN*), bone morphogenetic protein-2 (*BMP2*), and wingless-type 5a ligand (*Wnt5a*); **(B)** matrix and mineralization markers: collagen-type 1 (*Col1*), collagen-type 2 (*Col2*), and alkaline phosphatase (*ALP*); **(C)** osteoclastic recruitment markers: receptor activator of nuclear factor kappa-B ligand (*RankL*), and osteoprotegerin (*OPG*). Mean ± SD ($n = 3$). One-way ANOVA and *post-hoc* Tukey's multiple comparison test: $^{*}p < 0.05$, $^{\#}p < 0.01$, $^{\S}p < 0.001$; n.s. = not significant.

Osx expression, BM2-treated cells expressed high *BSP*, *BMP2*, and *Wnt5a*, whereas BM3 treatment resulted in a cell population represented by high expression of *Runx2*. On the other hand, culturing hPDCs in control medium, that is, GM′, induced cell populations that mainly had high *Col1* expression.

Characterization of the mineralized matrices on devitalized carriers

After devitalization, gross observation showed that the cellular structures of 3D hPDC cultures reduced in size and

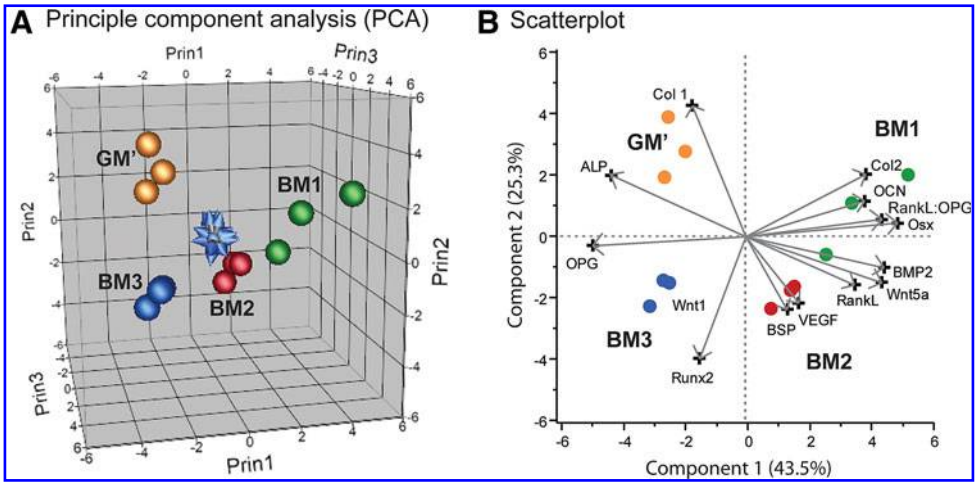

FIG. 3. Gene expression profiles of different cell populations after cultured in biomineralization media for 21 days *in vitro*. **(A)** Principle component analysis (PCA) showing the clustering of each samples under the same culture condition and separation of the clusters according to the treatments, and **(B)** their gene signatures visualized by the scatterplot.

shrunk upon drying down to the surface of the Ti-scaffolds as a relatively thin coating. Under brightfield microscopy, the mineralized matrices (indicated by *) were found covering the surface of the Ti-scaffolds at different degrees according to the type of BM used (Fig. 4A). In fact, BM3 resulted in the highest mineralized matrix deposition and homogeneity throughout the scaffolds, followed by BM2 and BM1 conditions, respectively. No mineralized matrix was found on the control media, that is, GM′. At higher magnification, these matrices showed a different morphology, varying from loose whitish patches (for BM1 and BM2) to a denser appearance (for BM3). Indeed, by SEM at high magnification (10,000×), agglomerates of mineralized matrix were revealed in the BM1 condition, whereas BM2 and BM3 resulted in the formation of a mineralized matrix either with plate-like crystals or aligned mineralized fibers, respectively (Fig. 4B).

The deposition of the mineralized matrices was evidenced by EDAX analysis, where calcium and phosphorus were found to be present within the matrices, whereas ECM formed under GM′ condition was not mineralized. These findings were further supported by the XRD analysis on the mineralized matrices, whereby peaks that are associated with hydroxyapatite (reference number: 00-024-0333) were found at $2\theta = 22.5°$, 25.9°, 28.3°, 31.7°, and 45.9° (indicated by ◆) (Fig. 4C). These peaks were absent in the nonmineralized matrices formed under GM′ condition. By Alizarin Red and Picro-Sirius Red stainings, the highest mineral and collagen contents were quantitated in samples derived from BM3 condition ($p < 0.05$ in both

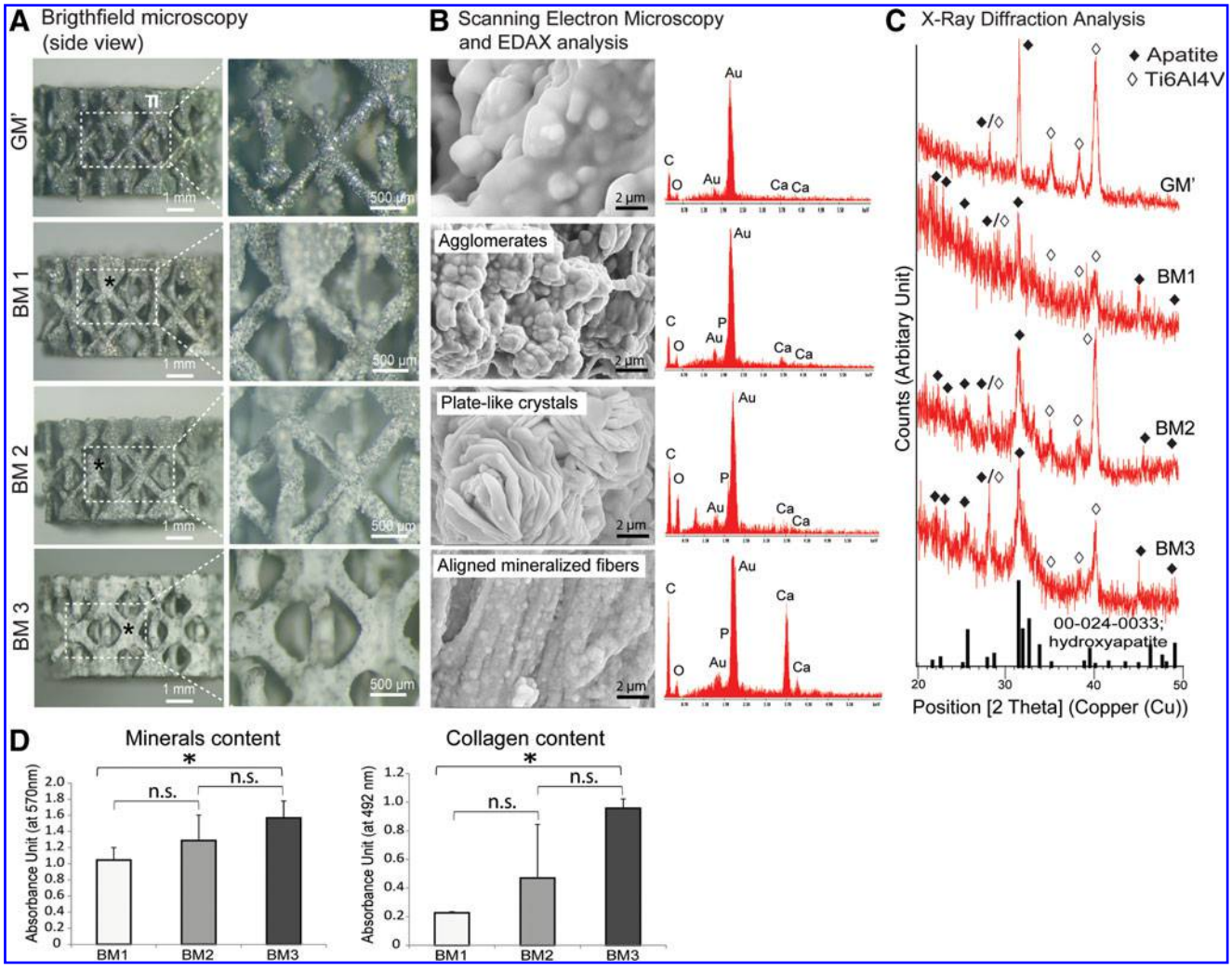

FIG. 4. Characterization of the deposited mineralized matrices on the devitalized carriers. **(A)** Representative brightfield microscopic images showing the morphology and distribution of the mineralized matrices that were deposited on the Ti-scaffolds. **(B)** By SEM (at 10,000 magnification), the mineralized matrices were revealed to have different morphology, varying from agglomerates to plate-like crystals and highly organized parallel mineralized fibers. EDAX analysis suggested the deposition of Ca^{2+} and PO_4^{3-} containing minerals. **(C)** XRD analysis confirmed the deposition of apatites indicated by the presence of peaks at 22.5°, 25.9°, 28.3°, 31,7°, and 45.9°. **(D)** Alizarin Red and Picro-Sirius Red staining and quantification showed the deposition of mineralized collagenous matrices on the porous Ti-scaffolds, with BM3 resulting in the highest mineralized matrix content. Mean ± SD ($n = 3$). Unpaired Student t-test (two-tailed): $*p < 0.05$; n.s. = not significant.

cases as compared to BM1), followed by BM2 and BM1 (Fig. 4D).

VEGF *gene expression and protein levels in the extracts of devitalized mineralized matrices*

As shown in Figure 5A, gene expression analysis revealed upregulation of *VEGF* expression by hPDCs after cultured in the three formulated BM for 21 days, whereby BM3 condition resulted in significantly higher gene expression than the control medium (i.e., GM′). However, no statistical difference in the gene expression levels between the three formulated BM was observed. Nevertheless, human-specific $VEGF_{165}$ subtype protein was detected in the extracts of the devitalized mineralized matrices by Western blotting, and quantification of the relative intensities (normalized to the intensities of GAPDH) showed that BM3 induced the highest protein expression, where the protein level by the BM2 condition was statistically not different from the GM′. No Western blot was performed for extract of the BM1 condition due to low amount of the extracted total proteins in the samples.

In vivo *ectopic bone induction by hPDC-reseeded, devitalized mineralized carriers*

After 8 weeks of subcutaneous implantation, nano-CT image analysis showed that all devitalized mineralized carriers induced ectopic bone formation (indicated as orange structures in pseudocolor or labeled as ''B''), except for the nonmineralized carriers obtained from the control condition, that is, GM′ (Fig. 6A). The newly formed bone was either in direct contact with the surface of the scaffold (labeled as ''Ti'') or formed bone ossicles that surrounded the scaffold struts. Nano-CT quantification revealed the highest bone volume induction by carriers obtained from the BM2 condition, followed by BM1, whereas carriers produced in the BM3 condition induced the lowest bone volume, which was significantly lower ($p < 0.05$) than that produced in BM2 (shown by the box-plots in Fig. 6B). However, none of the conditions induced homogeneous bone formation throughout the scaffolds as indicated by the sagittal, transaxial, and coronal planes of the 2D (Fig. 6C) and 3D (Fig. 6D) reconstructed nano-CT images.

The formed bone was found at discrete locations mainly at the top or bottom section of the scaffold (with columnar channels), and in lesser extent at the center section of the scaffold (with diamond unit cell). These findings were corroborated by histological staining of the resin-embedded sections using Stevenel's Blue and picrofuchsin solutions (Fig. 7), whereby bone (''B,'' stained in red color) was found either deposited on the scaffold surface or surrounding the scaffold struts. Interestingly, a bone marrow compartment (labeled as ''m'') in between the bone tissue and the scaffold was observed only on carriers obtained from BM2. No bone was observed in nonmineralized carriers (i.e., carriers produced in GM′); instead, only soft tissues (labeled as ''st'') was evidenced. Finally, no sign of inflammation or foreign body reaction was observed in any of the explants.

Discussion

In this study, we presented experimental data on the feasibility to produce devitalized osteoinductive mineralized carriers by functionalizing 3D porous scaffolds with an *in vitro* cell-made mineralized matrix under mineralizing culture conditions. Our ultimate goal is to produce off-the-shelf biomimetic mineralized carriers for autologous stem cell implantation in order to effectively mediate bone regeneration in the clinic. Indeed, there are established research findings evidencing the osteoinductivity of calcium phosphate-containing or mineralized biomaterials,[32,38,39] especially when the intramembranous ossification pathway is adopted as a bone engineering strategy.[40] Nevertheless, in order to achieve optimal bone-forming capacity, the type of calcium phosphate or mineralized matrix used is crucial to ensure a good match with the targeted cell type.[33,41] Therefore, it is a reasonable approach that if cells secrete and build their very-own mineralized matrix, this matrix will be more physiological and cell type-customized than a generic, synthetic matrix in terms of improving *in vivo* recognition, bone tissue induction, and implant integration into the host environment.[1,2,4]

In general, standard osteogenic medium that contains β-glycerophosphate (as mineral source) is used to promote mineralized ECM deposition *in vitro*. Although several recent studies have reported encouraging *in vitro* osteogenic differentiation effects, the *in vivo* bone-forming capacity

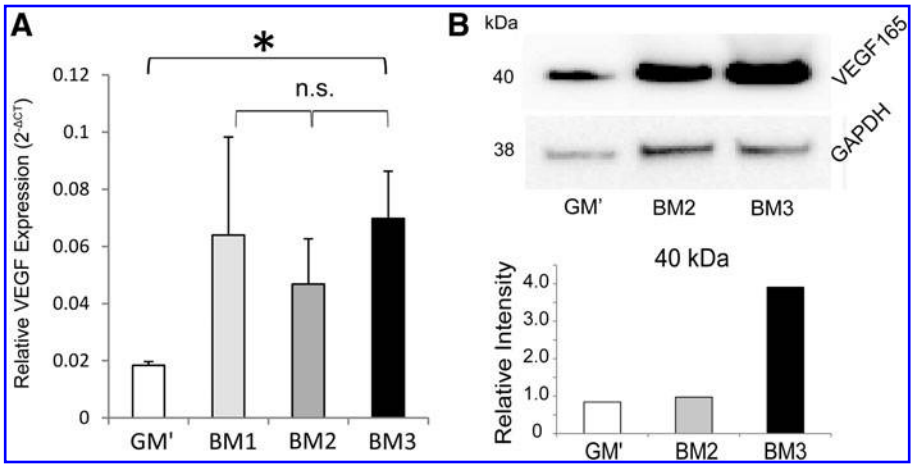

FIG. 5. **(A)** *VEGF* gene expression levels of hPDCs quantified by qRT-PCR after cultured in various BM for 21 days as compared to the control medium, GM′. Unpaired Student *t*-test (two-tailed): $*p < 0.05$; n.s. = not significant. **(B)** VEGF protein levels deposited in the mineralized matrix of the devitalized carriers obtained from various BM conditions by Western blot technique. qRT-PCR, quantitative real-time polymerase chain reaction.

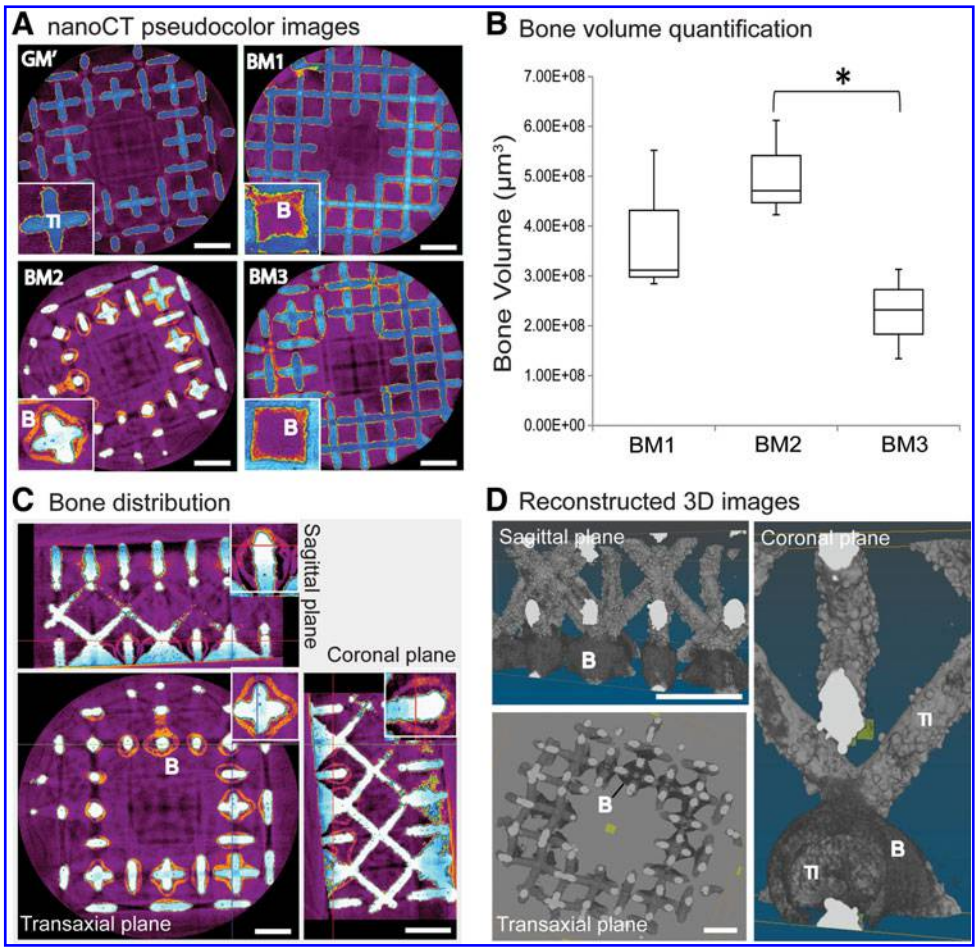

FIG. 6. *In vivo* ectopic osteoinduction by hPDC-reseeded devitalized mineralized carriers. **(A)** Nano-computed tomography (nano-CT) 2D images showing bone tissues (indicated as ''B'' for orange areas) formed on all the three formulated BM either deposited on or surrounded the scaffold struts (indicated as ''Ti'') (see insets). No bone formation was induced in the control condition, that is, GM′. **(B)** Box-plots showing highest bone volume was induced by carriers produced in BM2 condition, followed by BM1, and the lowest in BM3 as quantified by nano-CT analysis (unpaired Student *t*-test [two-tailed]: $*p < 0.05$; n.s. = not significant). **(C, D)** The sagittal, transaxial, and coronal planes of representative 2D and 3D reconstructed nano-CT images revealed inhomogeneous distribution of bone formation on the scaffolds, whereby the bone tissues were mainly found at the top or bottom section of the scaffold (with columnar channels) and in lesser extent at the center part of the scaffold (with diamond unit cell). Scale bar = 1 mm.

of these constructs was not apparent.[16,17] Based on this justification and our previous research findings on single ion-instructed cell proliferation and mineralized matrix formation,[34] we hypothesized that supplementing Ca^{2+} and PO_4^{3-} to a culture medium simultaneously would be favorable to the cells to self-modulate the uptake of the ions for mineralization of the cell-secreted ECM. The same opinion stands for studies that adopted an ion-enriched culture environment to direct nucleation of mineralizing ions onto the collagen fibers.[21,42]

In fact, our current findings clearly showed that cell proliferation was not compromised by the ions supplementation, and was significantly enhanced by adding ascorbic acid and further amplified by dexamethasone (which has been reported to induce a burst of proliferation in a cohort of cells that undergo differentiation[43]). This significant mitogenic effect also resulted in a complete closure of the scaffold pores where the highest cell proliferation was observed, indicating the feasibility to obtain carriers fully filled with cells and mineralized ECM. However, the deposited cellular structures reduced in size after devitalization and shrank to the surface of the Ti-scaffolds as a relatively thin coating upon drying, giving rise to an open porous mineralized carrier with minimal changes on the porosity and pore size. Nevertheless, this porous feature has crucial importance as a stem cell carrier to allow for high cell reseeding efficiency and to provide sufficient void volume for *in vivo* bone tissue formation inside the carrier.

Subsequently, we investigated the differentiation stage of hPDCs under the different mineralizing culture conditions through gene expression analysis. These data are of utmost importance as they provide information that reflects the osteogenicity of the deposited mineralized matrices due to different matrix compositions under the influences of the different culture media used. Specifically, addition of dexamethasone and ascorbic acid into the ion-supplemented medium (i.e., BM3) resulted in highly expressed *Runx2* but significantly lower *OCN*, *BSP*, and *BMP2* expressions.

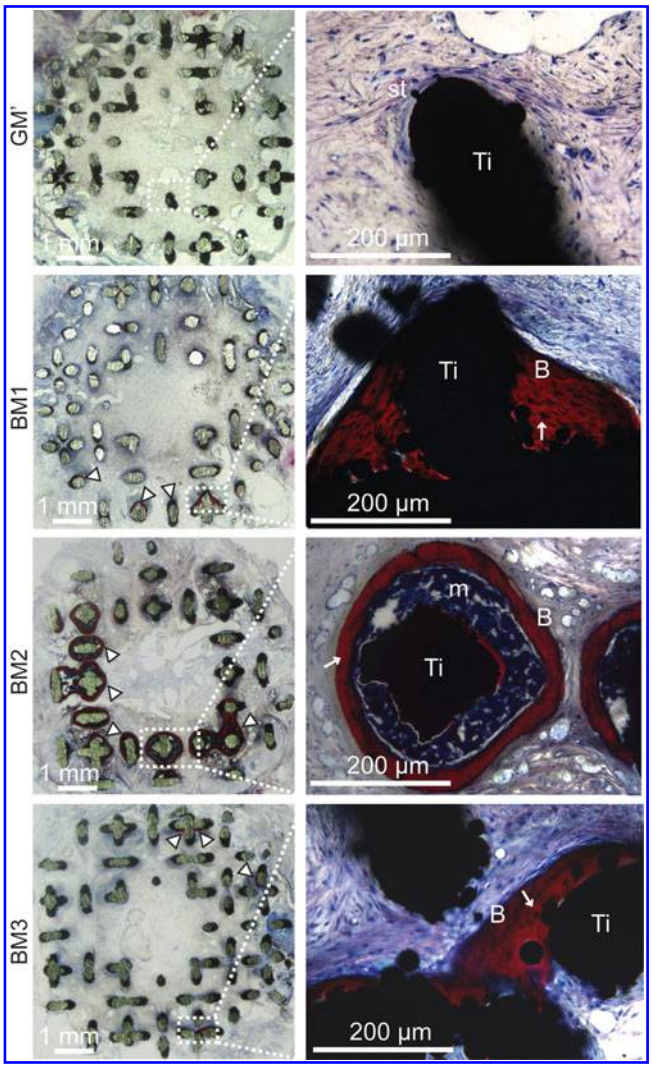

FIG. 7. Histological images showing bone tissue formation (indicated by *arrow heads* or labeled as ''B'') either in direct contact with the scaffold surface (labeled as ''Ti'') (in BM1 and BM3 conditions), or bone ossicles containing bone marrow (indicated as ''m'') surrounded the scaffold struts (in BM2 condition). Stevenel's Blue and picrofuchsin staining; st = soft tissues; ''↑'' indicates osteocytes.

This may indicate an enriching effect of osteochondroprogenitors on hPDCs by dexamethasone rather than differentiating the cells into a later stage of the osteogenic lineage.[44] Interestingly, no significant difference in Col2 expression (a chondrogenic matrix marker) was observed in this culture condition. Without dexamethasone, culturing hPDCs in ion-supplemented medium with ascorbic acid (i.e., BM2) resulted in a significant upregulation of *BSP* and *BMP2* expression, whereas purely ion-supplemented medium (i.e., BM1) may predispose the hPDCs toward a more advanced commitment in the osteogenic lineage as suggested by the upregulation of *Osx*.

It is known that *BSP*, consisting of 12% of the noncollagenous protein in human bone, acts as a nucleator of hydroxyapatite, and mediates cell metastasis on the bone surface via vitronectin receptor.[45] In fact, *BSP* deficiency impairs bone growth and mineralization, concomitant with dramatically reduced bone formation.[46] Similarly, *BMP2* expression (a potent bone inducer) was significantly upregulated in the BM2 condition, which may be another important contributor to the osteogenicity of the produced mineralized carriers. It is also interesting to observed that the up- and downregulation of *BMP2* expression coincided with the significant upregulation of *Osx* (activated upon BMP/p38 signaling[47]) in the BM1 and BM2 conditions, and the significant upregulation of *Runx2* in BM3 as *BMP2* was reported as a suppressor of *Runx2*.[48] Nevertheless, the observed *in vitro* gene expression responses were solely due to the different culture media formulations, whereas the *in vivo* bone formation outcomes could be influenced by various factors present on the produced mineralized carriers. These include the differences in substrate chemistry, surface roughness, porosity, as well as the cell–material–host interaction by the reseeded cells (such as implanted cell survival and differentiation into bone-forming cells *in vivo*, as well as their effect on early inflammation),[40,49] and the deposited proteins/growth factors.

Furthermore, the significant upregulation of *Wnt5a* ligand (associated to noncanonical Wnt-Ca^{2+} signaling) in the BM1 and BM2 conditions may be due to the Ca^{2+}-enriched culture environments. The biological effect of *Wnt5a* on osteogenic differentiation and bone formation is unclear.[50] For instance, Wnt5a has been reported to induce osteoblastogenesis in bone marrow MSCs,[51] but also to inhibit bone formation by promoting GSK-3-independent β-catenin degradation.[52] Interestingly, *Col1* expression was downregulated in all culture conditions, as well as the mineralization regulator, *ALP*. The downregulation of *ALP* could be attributed to a negative feedback on ALP expression under a high free PO_4^{3-} culture environment.[53] Both BM1 and BM2 conditions also induced significantly higher osteoclastic recruitment activity (as indicated by the increase in the *RanKL:OPG* ratio), probably a response by hPDCs in confrontation with a mineralizing culture condition.[40]

Finally, *VEGF* expression was upregulated in all BM conditions as compared to the control medium, and BM3 resulted in the most pronounced expression levels. This phenomenon could be related to the upregulation of *Runx2* under the BM3 condition, which has been reported as a necessary component for *VEGF* expression.[54] This finding was corroborated by the Western blot analysis whereby human-specific $VEGF_{165}$ subtype (an ECM-bound protein) was detected to be the highest in the extract of the mineralized matrix obtained from BM3.

The state-of-the-art decellularization method using a detergent was not adopted in this study, although it has been reported to be superior in obtaining a cell-/DNA-free ECM.[55,56] The main reason was to avoid any potential risk of denaturation of proteins or growth factors that might be secreted by the cells onto the mineralized matrix, which may be the key determinant(s) of osteoinduction of the produced carriers.[57] Therefore, a more gentle devitalization method was performed to lyse cells using three freeze–thaw cycles meanwhile preventing denaturation of the mineralized matrix and the secreted matrix-bound growth factors.[58] The use of different BM resulted in distinctly different mineral matrix morphologies (from agglomerates to plate-like and parallel mineralized fiber-like) as shown by brightfield microscopy and SEM. This is believed to be attributed to the use of ascorbic acid and/or dexamethasone that are both known to promote collagen synthesis, alkaline phosphatase

activity, and osteochondrogenic differentiation of hPDCs,[27] as well as their interactions with the supplemented Ca^{2+} and PO_4^{3-} ions.

Altogether, this might have resulted in different cell differentiation stages, different dynamics of the mineralization process, and different matrix compositions.[59,60] Different mineral morphologies could give rise to different physicochemical properties (including ion dissolution kinetics and surface roughness) that have been reported to have significant impact on *in vitro* cellular proliferation and differentiation as well as the *in vivo* osteoinductivity.[32,33] Unfortunately, assessment of the surface roughness by conventional technique such as atomic force microscopy on 3D scaffold[61] with limited flat surface is technically impossible. Furthermore, the deposited mineralized matrices were not homogenously distributed throughout the scaffolds; therefore, the assessment of surface roughness by other technique, such as computed tomography plus image analysis,[62] will not be representative. Thus, the effect of surface roughness on the biological outcomes could not be assessed in this study.

Encouragingly, reseeding hPDCs onto all devitalized, mineralized carriers induced ectopic bone formation after 8 weeks of implantation. By nano-CT image analysis and quantification, BM2 induced the highest bone volume, followed by BM1 and BM3. However, the percentage of bone formed within all the carriers was relatively low (approximately 0.5–1% of the total scaffold pore volume [$64.8 \pm 1.96\,mm^3$]). Inhomogeneous bone distribution within the scaffolds was most likely a result of inhomogeneity of mineralized matrix deposition (especially after devitalization), although a relatively high porosity and pore size of scaffold structure was used in this study under a shaking culture condition. This prompts the need to improve the mineralized matrix deposition throughout the scaffolds, for example, by perfusing BM through the scaffold in a controlled manner via a 3D perfusion bioreactor or by optimizing the scaffold properties through the study of the effect of the porous Ti-scaffold intrinsic properties (such as pore geometry, pore size, porosity, surface roughness, and chemistries) on mineralization of hPDCs.[63]

Additionally, we believe that the presence of bone–bone marrow entity formation in the BM2 condition could be related to the upregulation of *BMP2* expression, as BMP upregulation is associated with the observed bone-forming pattern.[64,65] This correlation can be further strengthened, as no bone marrow compartments were found by histological analysis in carriers produced by BM3, where *BMP2* expression was also significantly downregulated. The direct bone–titanium interface contacts indicated that *in vivo* biomechanical stability may be provided by the carriers to promote osseointegration.

Conclusions

In this study, we provided important biological insights on the effects of the studied BM on *in vitro* osteoprogenitor proliferation, osteogenic differentiation, and mineralized matrix deposition to functionalize 3D open porous scaffolds. Additionally, we demonstrated the feasibility to obtain devitalized mineralized carries that have different mineral morphologies and matrix composition, as well as a culture-dependent bone-forming capacity after reseeding hPDCs onto these carriers. This may represent a novel approach to produce highly biomimetic, mineralized tissue engineering constructs that hold potential as off-the-shelf stem cell carriers that could effectively mediate bone defect repair or regeneration in the clinic.

Acknowledgments

The authors thank Kathleen Bosmans and Carla Geeroms for their assistance on the subcutaneous implantation. This work is funded by the Research Foundation-Flanders (FWO: 1.5.172.13N—Interdisc.), FWO-ENDEAVOUR project (G.0982.11N), and Government Agency for Innovation by Science and Technology (IWT-111545), and is part of Prometheus, the Leuven Research & Development Division of Skeletal Tissue Engineering of the KU Leuven.

Author Disclosure Statement

No competing financial interests exist.

References

1. Ma PX. Biomimetic materials for tissue engineering. Adv Drug Deliv Rev. 2008;60:184–198.
2. Ingber DE, Mow VC, Butler D, et al. Tissue engineering and developmental biology: going biomimetic. Tissue Eng. 2006;12:3265–3283.
3. Grayson WL, Martens TP, Eng GM, et al. Biomimetic approach to tissue engineering. Semin Cell Dev Biol. 2009;20:665–673.
4. Benders KE, Weeren PR, Badylak SF, et al. Extracellular matrix scaffolds for cartilage and bone regeneration. Trends Biotechnol. 2013;13:169–176.
5. Badylak SF, Taylor D, Uygun K. Whole-organ tissue engineering: decellularization and recellularization of three-dimensional matrix scaffolds. Annu Rev Biomed Eng. 2011;13:27–53.
6. Arenas-Herrera JE, Ko IK, Atala A, Yoo JJ. Decellularization for whole organ bioengineering. Biomed Mater. 2013;8:014106.
7. Ott HC, Matthiesen TS, Goh SK, et al. Perfusion-decellularized matrix: using nature's platform to engineer a bioartificial heart. Nat Med. 2008;14:213–221.
8. Drosos GI, Kazakos KI, Kouzoumpasis P, Verettas DA. Safety and efficacy of commercially available demineralised bone matrix preparations: a critical review of clinical studies. Injury. 2007;38 Suppl 4:S13–S21.
9. Dinopoulos HT, Giannoudis PV. Safety and efficacy of use of demineralised bone matrix in orthopaedic and trauma surgery. Expert Opin Drug Saf. 2006;5:847–866.
10. Harakas NK. Demineralized bone-matrix-induced osteogenesis. Clin Orthopaed Relat Res. 1984;188:239–251.
11. Hinze MC, Wiedmann-Al-Ahmad M, Glaum R, et al. Bone engineering-vitalisation of alloplastic and allogenic bone grafts by human osteoblast-like cells. Br J Oral Maxillofac Surg. 2010;48:369–373.
12. Urist MR. Bone: formation by autoinduction. Science. 1965;150:893–899.
13. Datta N, Pham QP, Sharma U, et al. *In vitro* generated extracellular matrix and fluid shear stress synergistically enhance 3D osteoblastic differentiation. Proc Natl Acad Sci USA. 2006;103:2488–2493.
14. Pham QP, Kasper FK, Scott Baggett L, et al. The influence of an *in vitro* generated bone-like extracellular matrix on

osteoblastic gene expression of marrow stromal cells. Biomaterials. 2008;29:2729–2739.
15. Antebi B, Cheng X, Harris JN, et al. Biomimetic collagen-hydroxyapatite composite fabricated via a novel perfusion-flow mineralization technique. Tissue Eng Part C Methods. 2012;19:487–496.
16. Pham QP, Kasper FK, Mistry AS, et al. Analysis of the osteoinductive capacity and angiogenicity of an *in vitro* generated extracellular matrix. J Biomed Mater Res A. 2009; 88:295–303.
17. Sadr N, Pippenger BE, Scherberich A, et al. Enhancing the biological performance of synthetic polymeric materials by decoration with engineered, decellularized extracellular matrix. Biomaterials. 2012;33:5085–5093.
18. Boonrungsiman S, Gentleman E, Carzaniga R, et al. The role of intracellular calcium phosphate in osteoblast-mediated bone apatite formation. Proc Natl Acad Sci USA. 2012;109: 14170–14175.
19. Golub EE. Role of matrix vesicles in biomineralization. Biochim Biophys Acta. 2009;1790:1592–1598.
20. Liu Y, Kim YK, Dai L, et al. Hierarchical and non-hierarchical mineralisation of collagen. Biomaterials. 2011;32:1291–1300.
21. Colfen H. Biomineralization: a crystal-clear view. Nat Mater. 2010;9:960–961.
22. Thula TT, Rodriguez DE, Lee MH, et al. *In vitro* mineralization of dense collagen substrates: a biomimetic approach toward the development of bone-graft materials. Acta Biomater. 2011;7:3158–3169.
23. Barrere F, Layrolle P, van Blitterswijk CA, de Groot K. Biomimetic calcium phosphate coatings on Ti6AI4V: a crystal growth study of octacalcium phosphate and inhibition by Mg^{2+} and HCO_3. Bone. 1999;25:107S–111S.
24. Bigi A, Boanini E, Bracci B, et al. Nanocrystalline hydroxyapatite coatings on titanium: a new fast biomimetic method. Biomaterials. 2005;26:4085–4089.
25. Lopez-Heredia MA, Weiss P, Layrolle P. An electrodeposition method of calcium phosphate coatings on titanium alloy. J Mater Sci Mater Med. 2007;18:381–390.
26. Miao S, Weng W, Li Z, et al. Electrolytic deposition of octacalcium phosphate/collagen composite coating on titanium alloy. J Mater Sci Mater Med. 2009;20:131–134.
27. Tsui YC, Doyle C, Clyne TW. Plasma sprayed hydroxyapatite coatings on titanium substrates. Part 2: optimisation of coating properties. Biomaterials. 1998;19:2031–2043.
28. Fu Q, Hong Y, Liu X, et al. A hierarchically graded bioactive scaffold bonded to titanium substrates for attachment to bone. Biomaterials. 2011;32:7333–7346.
29. Nguyen HQ, Deporter DA, Pilliar RM, et al. The effect of sol-gel-formed calcium phosphate coatings on bone ingrowth and osteoconductivity of porous-surfaced Ti alloy implants. Biomaterials. 2004;25:865–876.
30. Wang D, Chen C, He T, Lei T. Hydroxyapatite coating on Ti6Al4V alloy by a sol-gel method. J Mater Sci Mater Med. 2008;19:2281–2286.
31. Landis WJ, Silver FH, Freeman JW. Collagen as a scaffold for biomimetic mineralization of vertebrate tissues. J Mater Chem. 2006;16:1495–1503.
32. Yuan H, Fernandes H, Habibovic P, et al. Osteoinductive ceramics as a synthetic alternative to autologous bone grafting. Proc Natl Acad Sci USA 2010;107:13614–13619.
33. Chai YC, Kerckhofs G, Roberts SJ, et al. Ectopic bone formation by 3D porous calcium phosphate-Ti6Al4V hybrids produced by perfusion electrodeposition. Biomaterials. 2012;33:4044–4058.
34. Chai YC, Roberts SJ, Van Bael S, et al. Multi-level factorial analysis of Ca2+/Pi supplementation as bio-instructive media for *in vitro* biomimetic engineering of three-dimensional osteogenic hybrids. Tissue Eng Part C Methods 2012;18:90–103.
35. Van Bael S, Chai YC, Truscello S, et al. The effect of pore geometry on the *in vitro* biological behavior of human periosteum-derived cells seeded on selective laser-melted Ti6Al4V bone scaffolds. Acta Biomater. 2012;8:2824–2834.
36. Eyckmans J, Luyten FP. Species specificity of ectopic bone formation using periosteum-derived mesenchymal progenitor cells. Tissue Eng. 2006;12:2203–2213.
37. Chai YC, Roberts SJ, Schrooten J, Luyten FP. Probing the osteoinductive effect of calcium phosphate by using an *in vitro* biomimetic model. Tissue Eng Part A. 2011;17: 1083–1097.
38. Bleek K, Taubert A. New developments in polymer-controlled, bio-inspired calcium phosphate mineralization from aqueous solution. Acta Biomater. 2013;9:6283–6321.
39. Sittichockechaiwut A, Scutt AM, Ryan AJ, et al. Use of rapidly mineralising osteoblasts and short periods of mechanical loading to accelerate matrix maturation in 3D scaffolds. Bone. 2009;44:822–829.
40. Chai YC, Roberts SJ, Desmet E, et al. Mechanisms of ectopic bone formation by human osteoprogenitor cells on CaP biomaterial carriers. Biomaterials. 2012;33:3127–3142.
41. Roberts SJ, Geris L, Kerckhofs G, et al. The combined bone forming capacity of human periosteal derived cells and calcium phosphates. Biomaterials. 2011;32:4393–4405.
42. Bradt JH, Mertig M, Teresiak A, Pompe W. Biomimetic mineralization of collagen by combined fibril assembly and calcium phosphate formation. Chem Mater. 1999;11:2694–2701.
43. McCulloch CA, Tenenbaum HC. Dexamethasone induces proliferation and terminal differentiation of osteogenic cells in tissue culture. Anat Rec. 1986;215:397–402.
44. Roberts SJ, Chen Y, Moesen M, et al. Enhancement of osteogenic gene expression for the differentiation of human periosteal derived cells. Stem Cell Res. 2011;7:137–144.
45. Ganss B, Kim RH, Sodek J. Bone sialoprotein. Crit Rev Oral Biol Med. 1999;10:79–98.
46. Malaval L, Wade-Gueye NM, Boudiffa M, et al. Bone sialoprotein plays a functional role in bone formation and osteoclastogenesis. J Exp Med. 2008;205:1145–1153.
47. Zilberberg L, ten Dijke P, Sakai LY, Rifkin DB. A rapid and sensitive bioassay to measure bone morphogenetic protein activity. BMC Cell Biol. 2007;8:41.
48. Komori T. Regulation of bone development and maintenance by Runx2. Front Biosci. 2008;13:898–903.
49. Chatterjea A, LaPointe VLS, Alblas J, et al. Suppression of the immune system as a critical step for bone formation from allogeneic osteoprogenitors implanted in rats. J Cell Mol Med. 2014;18:134–142.
50. Piters E, Boudin E, Van Hul W. Wnt signaling: a win for bone. Arch Biochem Biophys. 2008;473:112–116.
51. Takada I, Mihara M, Suzawa M, et al. A histone lysine methyltransferase activated by non-canonical Wnt signalling suppresses PPAR-gamma transactivation. Nat Cell Biol. 2007;9:1273–1285.
52. Topol L, Jiang X, Choi H, et al. Wnt-5a inhibits the canonical Wnt pathway by promoting GSK-3-independent beta-catenin degradation. J. Cell Biol. 2003;162:899–908.
53. Sapir-Koren R, Livshits G. Bone mineralization and regulation of phosphate homeostasis. IBMS BoneKEy. 2011;8:286–300.

54. Zelzer E, Glotzer DJ, Hartmann C, et al. Tissue specific regulation of VEGF expression during bone development requires Cbfa1/Runx2. Mech Dev. 2001;106:97–106.
55. Lu H, Hoshiba T, Kawazoe N, Chen G. Comparison of decellularization techniques for preparation of extracellular matrix scaffolds derived from three-dimensional cell culture. J Biomed Mater Res A. 2012;100:2507–2516.
56. He M, Callanan A. Comparison of methods for whole-organ decellularization in tissue engineering of bioartificial organs. Tissue Eng Part B Rev. 2012;19:194–208.
57. Crapo PM, Gilbert TW, Badylak SF. An overview of tissue and whole organ decellularization processes. Biomaterials. 2011;32:3233–3243.
58. Haykal S, Soleas JP, Salna M, et al. Evaluation of the structural integrity and extracellular matrix components of tracheal allografts following cyclical decellularization techniques: comparison of three protocols. Tissue Eng Part C Methods. 2012;18:614–623.
59. Langenbach F, Handschel J. Effects of dexamethasone, ascorbic acid and beta-glycerophosphate on the osteogenic differentiation of stem cells *in vitro*. Stem Cell Res Ther. 2013;4:117.
60. Nudelman F, Lausch AJ, Sommerdijk NA, Sone E.D. *In vitro* models of collagen biomineralization. J Struct Biol. 2013;183:258–269.
61. Serafim A, Mallet R, Pascaretti-Grizon F, et al. Osteoblast-like cell behavior on porous scaffolds based on poly(styrene) fibers. BioMed Res Int. 2014;2014:609319.
62. Kerchkhofs G, Pyka G, Papantoniou I, et al. High-resolution microfocus X-ray computed tomography for 3D surface roughness measurements of additive manufactured porous materials. Adv Eng Mater. 2013;15:153–158.
63. Thimm BW, Wust S, Hofmann S, et al. Initial cell precultivation can maximize ECM mineralization by human mesenchymal stem cells on silk fibroin scaffolds. Acta Biomater. 2011;7:2218–2228.
64. Wozney JM. Bone morphogenetic proteins. Prog Growth Factor Res. 1989;1:267–280.
65. Wozney JM. Overview of bone morphogenetic proteins. Spine (Phila Pa 1976). 2002;27:S2–S8.

Address correspondence to:
Jan Schrooten, PhD
Prometheus
Division of Skeletal Tissue Engineering
Department of Materials Engineering
KU Leuven
Kasteelpark Arenberg 44
Bus 2450
3001 Heverlee
Belgium

E-mail: jan.schrooten@mtm.kuleuven.be

Abbreviations Used

ANOVA = analysis of variance
BM = biomineralization medium
DBM = demineralized bone matrix
ECM = extracellular matrix
FBS = fetal bovine serum
hPDCs = human periosteal-derived progenitors
MSC = mesenchymal stem cell
Nano-CT = nano-computed tomography
PCA = principle component analysis
qRT-PCR = quantitative real-time polymerase chain reaction
XRD = X-ray diffraction